Mitigating Epilepsy by Stabilizing Linear Fractional-Order Systems

Emily A. Reed, Guilherme Ramos, Paul Bogdan, and Sérgio Pequito

***Abstract*— Epilepsy affects approximately 50 million people worldwide. Despite its prevalence, the recurrence of seizures can be mitigated only 70% of the time through medication. Furthermore, surgery success rates range from 30% - 70% because of our limited understanding of how a seizure starts. However, one leading hypothesis suggests that a seizure starts because of a critical transition due to an instability. Unfortunately, we lack a meaningful way to quantify this notion that would allow physicians to not only better predict seizures but also to mitigate them. Hence, in this paper, we develop a method to not only characterize the instability of seizures but also to leverage these conditions to stabilize the system underlying these seizures. Remarkably, evidence suggests that such critical transitions are associated with long-term memory dynamics, which can be captured by considering linear fractional-order systems. Subsequently, we provide for the first time tractable necessary and sufficient conditions for the global asymptotic stability of discrete-time linear fractional-order systems. Next, we propose a method to obtain a stabilizing control strategy for these systems using linear matrix inequalities. Finally, we apply our methodology to a real-world epileptic patient dataset to provide insight into mitigating epilepsy and designing future cyber-neural systems.**

I. Introduction

Epilepsy significantly inhibits the quality of life for approximately 50 million patients worldwide and results in \$16 billion in annual expenditures in the United States alone to treat [1]. Unfortunately, 15 million of those patients are unresponsive to medication [2], and surgery success rates are in the range of 30% - 70% due to our limited understanding of how and where the disease originates [3]. However, one leading hypothesis suggests that a seizure starts because of an instability in the brain [3], [4]. Leveraging this notion may lead to a better ability to not only predict seizures but also to mitigate them. However, stability criteria depend on the assumed mathematical description of the system [5], [6].

Many studies have opted to use linear dynamical models to describe the underlying neural dynamics exhibited in the brain [7], [8]; however, these models fail to capture the long-term memory clearly evidenced in neural signals [9], [10]. This inherent memory is characterized by the current state depending on an infinite combination of the previous states, where the absolute values of the weights on these previous states decay with time and are enclosed in an envelope that is described by a power law [11].

As an alternative to linear systems, fractional-order systems, which encapsulate this so-called long-term memory, have been shown to accurately represent neural behavior [12]–[14]. Furthermore, seizures in the brain can be characterized as critical shifts in dynamical behavior, which have been shown to correspond to an increase in long-term memory [15]. Therefore, considering the long-term memory of fractional-order systems and the stability of these systems may be beneficial in assessing, predicting, and mitigating seizures. From here on, we focus on the stability of fractional-order systems and the stabilization of these systems as a mechanism to mitigate seizures in the brain.

The recent survey on fractional cyber-neural systems in [16] overviews all of the stability results pertaining to fractional-order systems. In this paper, we focus on discrete-time systems since the measurements of neural behavior are inherently discrete in nature. While recent work has investigated conditions for the stability of discrete-time linear fractional-order systems (DTLFOS) [17], these conditions are not tractable for analysis let alone for design as they are dependent on each time step. Therefore, tractable stability conditions for DTLFOS do not currently exist. Thus, we provide the following three main contributions.

Main contributions: *(1)* We provide tractable necessary and sufficient conditions for the global asymptotic stability of discrete-time linear fractional-order systems. *(2)* We develop a computationally efficient framework to stabilize linear fractional-order dynamical networks. *(3)* We demonstrate the validity of our proposed mathematical formalism by considering a comprehensive real-world epileptic dataset and provide a novel understanding of new treatments for epilepsy.

II. Problem Statement

In this paper, we consider (non-commensurate) discrete-time linear fractional-order systems (DTLFOS) described by

$$\Delta^{\alpha} x[k+1] = Ax[k], \tag{1}$$

where $k \in \mathbb{N}$ is the time step, $x[k] \in \mathbb{R}^n$ denotes the state, $A \in \mathbb{R}^{n\times n}$ is the coupling matrix that describes the spatial relationship between different states, $\alpha \in \mathbb{R}^n$ are the fractional-order exponents that capture the long-term memory in the system, and Δ^{α} is the Grünwald-Letnikov discretization of the fractional derivative (Chpt.1, [18]). For any i-th state ($1 \leq i \leq n$), we can express $\Delta^{\alpha_i} x_i[k] = \sum_{j=0}^{k} \psi(\alpha_i, j) x_i[k-j]$, where $\alpha_i \in \mathbb{R}$ is the fractional-order exponent of the ith state and $\psi(\alpha_i, j) = \frac{\Gamma(j-\alpha_i)}{\Gamma(-\alpha_i)\Gamma(j+1)}$, with $\Gamma(\cdot)$ denoting the Gamma function [19]. From here onward, we will use the tuple (A, α) to represent the DTLFOS (1).

The fractional-order exponents determine the weights on the previous states that are needed to compute the next state. These weights decay as a power law. As the fractional-order exponents approach zero, the next state depends less on states in the distant past and ultimately become LTI if

E. A. Reed and P. Bogdan are with Ming Hsieh Electrical and Computer Engineering Department, University of Southern California, USA emilyree@usc.edu, pbogdan@usc.edu

G. Ramos is with Dept. of Computer Science and Engineering, Instituto Superior Técnico, University of Lisbon, Portugal and Instituto de Telecomunicações, 1049-001 Lisbon, Portugal. guilherme.ramos@tecnico.ulisboa.pt

S. Pequito is with the Division of Systems and Control, Department of Information Technology, Uppsala University, Uppsala, Sweden sergio.pequito@it.uu.se

all exponents are equal to zero [11]. Thus, when learned, if the exponents are significantly different from zero, then the system is inherently *not* an LTI system.

Next, we recall the generic definition of global asymptotic stability (Definition 5.4.1, [6]). Specifically, a DTLFOS (1) is globally asymptotically stable (g.a.s.) when the following two conditions hold: *(1)* for every $\varepsilon > 0$ and $k_0 \in \mathbb{N}$, there exists $\delta = \delta(\varepsilon, k_0) > 0$ such that for every $x[k_0] \in \mathbb{R}^n$ if $\|x[k_0]\|_2 < \delta$, then $\|x[k]\|_2 < \varepsilon$ for all $k \geq k_0$, and *(2)* $\lim_{k\to\infty} \|x[k]\|_2 = 0$, where $\|\cdot\|_2$ is the Euclidean norm.

As previously mentioned, it is believed that a seizure starts because of a critical transition due to an instability [3], [4]. Under this assumption, we seek to develop methods to stabilize the behavior of the brain as a means to mitigate seizures. As a proxy to brain behavior, we consider sampled neural recordings (i.e., intracranial electrocortiography) and model them as a DTLFOS–for which we later provide evidence to be a suitable model. That said, towards stabilization, one approach is to alter the interconnections between different states, which could represent the inter-dependencies among neuronal populations. Thus, we introduce the first problem as follows: given (A, α), find a coupling matrix $\tilde{A}$ that satisfies the following

$$\begin{aligned} \underset{\tilde{A}\in\mathbb{R}^{n\times n}}{\text{minimize}} \quad & \|\tilde{A}\|_0 \\ \text{s.t.} \quad & (A+\tilde{A}, \alpha) \text{ is globally} \\ & \text{asymptotically stable,} \end{aligned} \qquad (\mathbf{P}_1)$$

where $\|\cdot\|_0$ represents the zero quasi-norm, which measures the number of non-zero entries in a matrix or vector. If $\alpha = 0$, then we would be dealing with a LTI system, and the problem could be solved using the methods in [20], [21]. Yet, when $\alpha \neq 0$, we wonder if it is possible to alter the fractional-order exponents to achieve stability. This leads us to introduce the following problem: given (A, α), find the fractional-order exponents $\tilde{\alpha}$ that satisfies the following

$$\begin{aligned} \underset{\tilde{\alpha}\in\mathbb{R}^{n}}{\text{minimize}} \quad & \|\tilde{\alpha}\|_0 \\ \text{s.t.} \quad & (A, \alpha+\tilde{\alpha}) \text{ is globally} \\ & \text{asymptotically stable.} \end{aligned} \qquad (\mathbf{P}_2)$$

Notice that this problem is somewhat unconventional. It means that we may be able to change the memory dependency of specific brain regions, which then suggests that the lack of asymptotic stability is the result of either too much or too little integration of the memory in a neural region.

III. STABILIZING DTLFOS

In Section III-A, we show the necessary and sufficient conditions for the g.a.s. of DTLFOS. In Section III-B, we convexify $\mathbf{P}_1$ and $\mathbf{P}_2$ and give convexified solutions in Section III-C. Finally, in Section III-D, we provide sufficient yet computationally efficient solutions to $\mathbf{P}_1$ and $\mathbf{P}_2$. All proofs are relegated to the Appendix.

A. Necessary and Sufficient Conditions for Global Asymptotic Stability of DTLFOS

In contrast with the conditions given in [17], we provide a closed-form solution to assess the g.a.s. of DTLFOS.

Theorem 1: A non-commensurate DTLFOS (1) is said to be g.a.s. *if and only if* for $A_0 := A - D(\alpha, 1)$, where $D(\alpha, j) = \begin{bmatrix} \psi(\alpha_1,j) & 0 & \dots & 0 \\ 0 & \psi(\alpha_2,j) & \dots & 0 \\ & \vdots & \ddots & \\ 0 & \vdots & & 0 \\ 0 & 0 & \dots & \psi(\alpha_n,j) \end{bmatrix}$, we have $|\lambda| < 1$ for all $\lambda \in \sigma(A_0)$, where $\sigma(A_0)$ is the set of eigenvalues of matrix A_0.

B. Convexification of $\mathbf{P}_1$ and $\mathbf{P}_2$

By invoking Theorem 1, we can rewrite $\mathbf{P}_1$ and $\mathbf{P}_2$ as

$$\begin{aligned} \underset{\tilde{A}\in\mathbb{R}^{n\times n}}{\text{minimize}} \quad & \|\tilde{A}\|_0 \\ \text{s.t.} \quad & \rho(A+\tilde{A}-D(\alpha,1)) < 1, \end{aligned} \qquad (\mathbf{P}_1)$$

and

$$\begin{aligned} \underset{\tilde{\alpha}\in\mathbb{R}^{n}}{\text{minimize}} \quad & \|\tilde{\alpha}\|_0 \\ \text{s.t.} \quad & \rho(A-D(\alpha+\tilde{\alpha},1)) < 1, \end{aligned} \qquad (\mathbf{P}_2)$$

where $\rho(M) := \max\{|\lambda| : \lambda \in \sigma(M)\}$ is the spectral radius, which is the largest eigenvalue in magnitude of an arbitrary matrix $M \in \mathbb{R}^{n\times n}$.

Unfortunately, the objective functions of $\mathbf{P}_1$ and $\mathbf{P}_2$ are nonconvex, so we propose a convexification by considering the sparsity promoting $1-$norm [22]. Specifically, we obtain respectively, the following objectives for both problems:

$$\begin{aligned} \underset{\tilde{A}\in\mathbb{R}^{n\times n}}{\text{minimize}} \quad & \|\tilde{A}\|_1 \\ \text{s.t.} \quad & \rho(A+\tilde{A}-D(\alpha,1)) < 1, \end{aligned} \qquad (\mathbf{P}_1^c)$$

and

$$\begin{aligned} \underset{\tilde{\alpha}\in\mathbb{R}^{n}}{\text{minimize}} \quad & \|\tilde{\alpha}\|_1 \\ \text{s.t.} \quad & \rho(A-D(\alpha+\tilde{\alpha},1)) < 1. \end{aligned} \qquad (\mathbf{P}_2^c)$$

C. Solutions to $\mathbf{P}_1^c$ and $\mathbf{P}_2^c$

Next, we present the solutions to $\mathbf{P}_1^c$ and $\mathbf{P}_2^c$.

Proposition 1: The solution to $\mathbf{P}_1^c$ is given by

$$\tilde{A} = L_1 P_1^{-1}, \qquad (2)$$

where P_1 and L_1 are found by solving the following convex optimization problem:

$$\begin{aligned} \underset{P_1\in\{P_1\in\mathbb{R}^{n\times n}:P_1>0\}, L_1\in\mathbb{R}^{n\times n}}{\text{minimize}} \quad & \|P_1\|_1 + \|L_1\|_1 \\ \text{s.t.} \quad & \begin{bmatrix} P_1 & P_1 A_0^\intercal + L_1^\intercal \\ A_0 P_1 + L_1 & P_1 \end{bmatrix} > 0. \end{aligned}$$

In contrast, the solution to $\mathbf{P}_2^c$ is as follows.

Proposition 2: A suboptimal solution to $\mathbf{P}_2^c$ is given by

$$\tilde{\alpha}_i = \Gamma(2)(L_2 P_2^{-1})_{i,i} - \alpha_i \qquad (3)$$

for all $i \in \{1, \ldots, n\}$, where P_2 and L_2 are found by solving the following convex optimization problem:

$$\underset{P_2 \in \{P_2 \in \mathbb{R}^{n\times n}: P_2 > 0\}, L_2 \in \mathbb{R}^{n\times n}}{\text{minimize}} \|P_2\|_1 + \|L_2\|_1$$
$$\text{s.t.} \begin{bmatrix} P_2 & P_2 A^\intercal + L_2^\intercal \\ AP_2 + L_2 & P_2 \end{bmatrix} > 0 \text{ and } P_2, L_2 \text{ diagonal.}$$

Notice that in contrast with the solution to $\mathbf{P}_1^c$, in the suboptimal solution to $\mathbf{P}_2^c$, we only alter the elements of $\tilde{\alpha}$ to be possibly nonzero. In turn, $\tilde{\alpha}$ corresponds to the diagonal entries of $L_2 P_2^{-1}$ that in all likelihood are only numerically possible when both matrices L_2 and P_2 are restricted to be diagonal and P_2 is positive definite.

D. Computationally Efficient and Graphically-Interpretable Sufficient Approximate Solutions for $\mathbf{P}_1^c$ and $\mathbf{P}_2^c$

In this section, we present graphically-interpretable sufficient approximate solutions to solve $\mathbf{P}_1^c$ and $\mathbf{P}_2^c$.

Proposition 3: The following problem formulation is sufficient for solving $\mathbf{P}_1^c$:

$$\begin{aligned} &\underset{\tilde{A} \in \mathbb{R}^{n\times n}}{\text{minimize}} \quad \|\tilde{A}\|_1 \\ &\text{s.t.} \left| a_{i,i} + \tilde{a}_{i,i} + \frac{\alpha_i}{\Gamma(2)} \right| < 1 - \sum_{j \in N\setminus\{i\}} |a_{i,j} + \tilde{a}_{i,j}|. \end{aligned} \tag{$\mathbf{P}_1^g$}$$

Similarly, we present the graphically-interpretable sufficient approximate solution for $\mathbf{P}_2^c$.

Proposition 4: The following problem formulation is sufficient for solving $\mathbf{P}_2^c$:

$$\begin{aligned} &\underset{\tilde{\alpha} \in \mathbb{R}^{n}}{\text{minimize}} \quad \|\tilde{\alpha}\|_1 \\ &\text{s.t.} \left| a_{i,i} + \frac{(\alpha_i + \tilde{\alpha}_i)}{\Gamma(2)} \right| < 1 - \sum_{j \in N\setminus\{i\}} |a_{i,j}|. \end{aligned} \tag{$\mathbf{P}_2^g$}$$

We remark that these solutions are more computationally efficient as there is only a single $(n \times n)$ matrix in the case of $\mathbf{P}_1^g$ and a single vector of size n in the case of $\mathbf{P}_2^g$ that need to be found, whereas in $\mathbf{P}_1^c$ and $\mathbf{P}_2^c$ two $(n \times n)$ matrices must be found. Furthermore, $\mathbf{P}_1^c$ has $4n^2$ constraints and $\mathbf{P}_2^c$ has $6n^2 - 4n$ constraints, whereas both $\mathbf{P}_1^g$ and $\mathbf{P}_2^g$ only have n constraints. These sufficient approximate solutions are advantageous in the context of epilepsy as there may be many sensors to measure brain activity, so the network may be very large. Furthermore, they enable neuroscientists and physicians with criteria that are graphically intuitive.

IV. Mitigating Epilepsy

We illustrate the usefulness of our framework by applying it to a dataset from an epileptic patient [23]. Specifically, we unveil new insights into novel treatments for epilepsy.

We studied the first 6 channels of electrocorticography data from patient HUP64 ictal block 1 in the International Epilepsy Electrophysiology Portal [23]. The data was recorded at a sampling rate of 512 Hz, it was marked by clinical experts, and it was pre-processed according to the procedure outlined in [7]. We verified that the data exhibits long-range dependence by computing the Hurst exponents for each channel $\{0.66, 0.66, 0.77, 0.72, 0.75, 0.7\}$, which motivates the use of a DTLFOS as a suitable model for the data [24]. Next, we estimated the parameters of DTLFOS, namely the coupling matrix A and the fractional-order exponents α, from the data using the methods in [25] and a time window of 1 second. We then examined the parameters 12 seconds before the seizure in Figs. 1 (a) and (b), and during the seizure, specifically, 48 seconds after its start, in Figs. 3 (a) and (b).

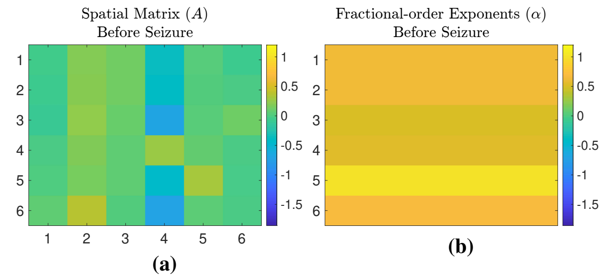

Fig. 1: Spatial matrix and fractional-order exponents 12 seconds before the patient's seizure.

Epileptic Data

By Theorem 1, we find that both systems (before and during the seizure), are unstable, yet with different dynamical properties, as captured by the systems' eigenvalues before and during the seizure, see Fig. 2 (a) and (b), respectively.

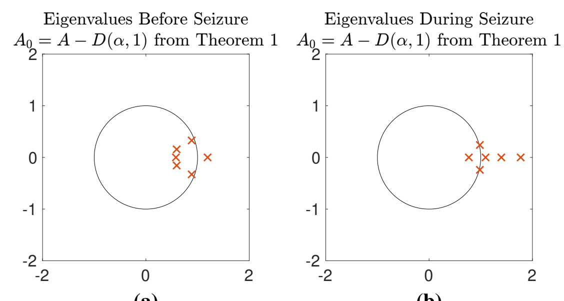

Fig. 2: Eigenvalues of $A_0 = A - D(\alpha, 1)$ are shown as red crosses and depicted in the complex plane using the DTLFOS parameters 12 seconds before and 48 seconds after the seizure starts.

Next, to stabilize the DTLFOS during the seizure, we solve $\mathbf{P}_1^c$ and $\mathbf{P}_2^c$ as proposed in Proposition 1 and Proposition 2, respectively, using CVX in MATLAB [26] and the parameters during the seizure. We present the results in Fig. 3.

On the one hand, after solving $\mathbf{P}_1^c$, the diagonal values of $\tilde{A}$ and the updated spatial matrix $A + \tilde{A}$ are lower as compared to the diagonal values of A as shown in Figs. 3 (a), (c), and (e). Here, we can interpret the spatial matrix as the level of activity between neuron populations. Therefore, having lower values might indicate that there is less activity between neuron populations.

On the other hand, after solving $\mathbf{P}_2^c$, we notice that the values of the altered $\tilde{\alpha}$ and updated fractional-order exponents $\alpha + \tilde{\alpha}$ are, in general, lower than the values of α as shown in Figs. 3 (b), (d), and (f). The original fractional-order exponents (α) during the seizure are close to 1. However, the updated fractional-order exponents have lower values in the range of $(-0.6, 0.5)$, which provides converging evidence for the empirical results presented in [15].

After solving $\mathbf{P}_1^c$ and $\mathbf{P}_2^c$, we find the eigenvalues for the new systems as shown in Figs. 3 (g) and (h), which verify the feasibility of our problems by invoking Theorem 1.

Finally, for illustration, we obtain the solutions to $\mathbf{P}_1^g$ and $\mathbf{P}_2^g$ given by Proposition 3 and Proposition 4, respectively, depicted in Fig. 4. We again find that the diagonal values of the new spatial matrix are lower than the diagonal values of A. Similarly, the values of the new fractional-order exponents are lower than the values of α. Once again, feasibility is ensured by invoking Theorem 1.

Discussion

In this section, we analyze the implications that our framework has on providing potential treatments for epilepsy. We notice in Fig. 2 that while both systems before and during the seizure are unstable, in the case of the system during the seizure, there are more eigenvalues outside of the unit circle. This might indicate that the system moves further from stability during seizure [3], [4]. Therefore, to mitigate the seizure, it is hypothesized that we must correct for instability [3], [4]. Our framework achieves this by either altering the fractional-order exponents or the spatial matrix.

In practice, changing the system parameters could be achieved through the target release of a drug [27], electrical or ultrasound neurostimulation [28], optogenetics [29], or even through the regulation of the glia astrocytes [30]. Our method is an event-triggered state-feedback control, i.e., $u[k] = Kx[k]$, where $u[k]$ is the control input, and it is employed when a seizure is detected. For example, in the case of $\mathbf{P}_1^c$, this is as simple as setting $K = \tilde{A}$. For $\mathbf{P}_2^c$, we simply set the diagonal entries of $K_{i,i} = \frac{-\tilde{\alpha}_i}{\Gamma(2)}$ for all $i \in \{1, \ldots, n\}$, and the off-diagonal entries are zero.

V. Conclusions and Future Works

We provided computationally efficient necessary and sufficient conditions for the stability of discrete-time linear fractional-order systems. Leveraging these conditions, we developed a framework using linear matrix inequalities to stabilize fractional-order systems. We applied our framework to a real-world dataset of an epileptic patient to show that we can impose stability on these systems with the hope that these methods will lead to the development of effective future treatments of epilepsy and other neurological diseases.

More work is needed to study larger datasets in depth to understand and verify the dependence between the DTLFOS stability and the seizure onset. Previous work has examined this relationship for switched linear systems [7], but future work is needed to rigorously examine this notion for fractional-order systems. Future work also includes developing a framework that can simultaneously design both parameters of the fractional-order systems – the fractional-order exponents and the spatial matrix – to ensure stability.

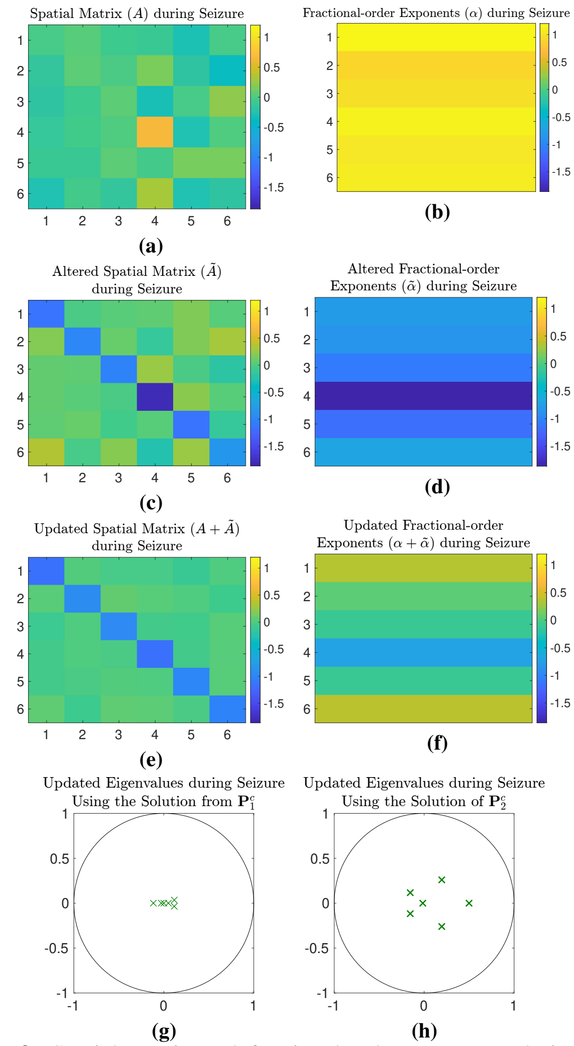

Fig. 3: Spatial matrix and fractional-order exponents during the seizure, and their updated values and updated eigenvalues (shown in green crosses on the complex plane) after solving $\mathbf{P}_1^c$ and $\mathbf{P}_2^c$.

VI. Acknowledgements

Emily A. Reed gratefully acknowledges the support from the National Science Foundation GRFP DGE-1842487, the University of Southern California Annenberg Fellowship, and a USC WiSE Top-Off Fellowship.

Paul Bogdan and Emily A. Reed gratefully acknowledge the support by the National Science Foundation under the Career Award CPS/CNS-1453860, the NSF award under Grant Numbers CCF-1837131, MCB-1936775, CMMI-1936624, and CNS-1932620, the

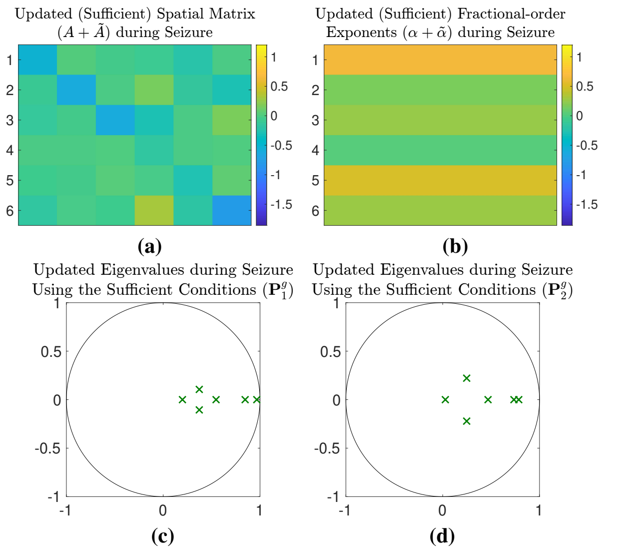

Fig. 4: These figures show the updated spatial matrix, fractional-order exponents, and eigenvalues (shown in green crosses on the complex plane) after solving $\mathbf{P}_1^g$ and $\mathbf{P}_2^g$.

U.S. Army Research Office (ARO) under Grant No. W911NF-17-1-0076 and W911NF-23-1-0111, and the DARPA Young Faculty Award and DARPA Director Award, under Grant Number N66001-17-1-4044, a 2021 USC Stevens Center Technology Advancement Grant (TAG) award, an Intel faculty award and a Northrop Grumman grant.

The financial supporters of this work had no role in the study design, data collection and analysis, decision to publish, or preparation of the manuscript. The views, opinions, and/or findings contained in this article are those of the authors and should not be interpreted as representing official views or policies, either expressed or implied by the Defense Advanced Research Projects Agency, the Department of Defense or the National Science Foundation.

VII. APPENDIX

Proof of Theorem 1: To present the global asymptotic stability conditions of the non-commensurate DTLFOS, we start by re-writing the DTLFOS in (1) as $x[k+1] = \sum_{j=0}^{k} A_j x[k-j]$, where $A_0 = A - D(\alpha, 1)$, $A_j = -D(\alpha, j+1)$, for $j \geq 1$, and

$$D(\alpha, j) = \begin{bmatrix} \psi(\alpha_1, j) & 0 & \dots & 0 \\ 0 & \psi(\alpha_2, j) & \dots & 0 \\ & \vdots & \ddots & \\ 0 & & & 0 \\ 0 & 0 & \dots & \psi(\alpha_n, j) \end{bmatrix}, \tag{4}$$

by invoking Lemma 2 in [25]. Next, we can re-write it as

$$\begin{bmatrix} x[1] \\ x[2] \\ x[3] \\ \vdots \end{bmatrix} = \underbrace{\begin{bmatrix} A_0 & 0 & 0 & 0 & \dots \\ A_1 & A_0 & 0 & 0 & \dots \\ A_2 & A_1 & A_0 & 0 & \dots \\ \vdots & \vdots & \vdots & \vdots & \ddots \end{bmatrix}}_{\mathcal{A}} \begin{bmatrix} x[0] \\ x[1] \\ x[2] \\ \vdots \end{bmatrix}. \tag{5}$$

We observe that the system in (5) is an infinite-dimensional linear time-invariant system described by an operator $\mathcal{A}$.

We start by noticing that the dimension of $\mathcal{A}$ is countably infinite since it is described by a countably infinite set of finite-dimensional matrices. So, the point spectrum of $\mathcal{A}$ is countably infinite.

Next, we consider the point spectrum of the operator $\mathcal{A}$, denoted by $\operatorname{spec}(\mathcal{A}) = \operatorname{spec}\left(\begin{bmatrix} A_0 & 0 & 0 & \dots \\ A_1 & A_0 & 0 & \dots \\ A_2 & A_1 & A_0 & \dots \\ \vdots & \vdots & \vdots & \ddots \end{bmatrix}\right) = \sigma(A_0) \bigcup \operatorname{spec}\left(\begin{bmatrix} A_0 & 0 & 0 & \dots \\ A_1 & A_0 & 0 & \dots \\ A_2 & A_1 & A_0 & \dots \\ \vdots & \vdots & \vdots & \ddots \end{bmatrix}\right)$, where the second equality is a consequence of the properties of matrix determinants and the Leibniz expansion. By induction and Theorem 2.12 in [31], it readily follows that $\operatorname{spec}(\mathcal{A}) = \bigcup^{\infty} \sigma(A_0)$, where the symbol ∞ indicates the union of a countable collection of sets. Subsequently, it follows that $\operatorname{spec}(\mathcal{A}) = \sigma(A_0)$. Therefore, by the definition of g.a.s. and the stability conditions stated in Theorem 8.3 in [5], the DTLFOS is g.a.s. when $|\lambda| < 1, \forall \lambda \in \sigma(A_0)$.

Proof of Proposition 1: To solve $\mathbf{P}_1^c$, we notice that by invoking Theorem 8.4 in [5], $\mathbf{P}_1^c$ can be restated as

$$\begin{aligned} &\underset{P_1 \in \{P_1 \in \mathbb{R}^{n\times n} : P_1 > 0\}, \tilde{A} \in \mathbb{R}^{n \times n}}{\text{minimize}} && \|\tilde{A}\|_1 \\ &\text{s.t. } (A_0 + \tilde{A})^\intercal P_1 (A_0 + \tilde{A}) - P_1 < 0. \end{aligned} \tag{$\mathbf{P}_1$}$$

By applying Theorem 3 in [21], the problem becomes

$$\begin{aligned} &\underset{P_1 \in \{P_1 \in \mathbb{R}^{n\times n} : P_1 > 0\}, L_1 \in \mathbb{R}^{n \times n}}{\text{minimize}} && \|P_1\|_1 + \|L_1\|_1 \\ &\text{s.t. } \begin{bmatrix} P_1 & P_1 A_0^\intercal + L_1^\intercal \\ A_0 P_1 + L_1 & P_1 \end{bmatrix} > 0, \end{aligned} \tag{$\mathbf{P}_1^c$}$$

where $\tilde{A} = L_1 P_1^{-1}$. Since $\mathbf{P}_1^c$ is convex, it can be easily solved for L_1 and P_1 by using the interior points method [32].

Proof of Proposition 2: Similarly to Proposition 1, we begin to solve $\mathbf{P}_2^c$. Hence, by Theorem 8.4 in [5], we can restate $\mathbf{P}_2^c$ as

$$\begin{aligned} &\underset{P_2 \in \{P_2 \in \mathbb{R}^{n\times n} : P_2 > 0\}, \tilde{\alpha} \in \mathbb{R}^{n}}{\text{minimize}} && \|\tilde{\alpha}\|_1 \\ &\text{s.t. } (A - D(\alpha + \tilde{\alpha}, 1))^\intercal P_2 (A - D(\alpha + \tilde{\alpha}, 1)) - P_2 < 0. \end{aligned} \tag{$\mathbf{P}_2^c$}$$

We again apply Theorem 3 in [21] to obtain the following

$$\begin{aligned} &\underset{P_2 \in \{P_2 \in \mathbb{R}^{n\times n} : P_2 > 0\}, L_2 \in \mathbb{R}^{n \times n}}{\text{minimize}} && \|P_2\|_1 + \|L_2\|_1 \\ &\text{s.t. } \begin{bmatrix} P_2 & P_2 A^\intercal + L_2^\intercal \\ A P_2 + L_2 & P_2 \end{bmatrix} > 0, \end{aligned} \tag{$\mathbf{P}_2^c$}$$

where $D(\alpha + \tilde{\alpha}, 1) = -L_2 P_2^{-1}$. Since $D(\alpha + \tilde{\alpha}, 1)$ is diagonal, we restrict L_2 and P_2 to be diagonal, which imposes $2(n^2 - n)$ additional linear constraints. $\mathbf{P}_2^c$ is convex and can be solved for L_2 and P_2 by using the interior points method [32]. From $D(\alpha + \tilde{\alpha}, 1) = -L_2 P_2^{-1}$, we need a way to easily obtain $\tilde{\alpha}$.

From (4), we notice that $D(\alpha + \tilde{\alpha}, 1)$ is dependent on $\psi(\alpha_i + \tilde{\alpha}_i, 1) = \frac{\Gamma(1 - (\alpha_i + \tilde{\alpha}_i))}{\Gamma(-(\alpha_i + \tilde{\alpha}_i))\Gamma(2)}$ for all $i \in \{1, \dots, n\}$. Yet, remarkably, from the relationship $\Gamma(1+z) = z\Gamma(z)$, we have that $\psi(\alpha_i + \tilde{\alpha}_i, 1)$ can be simplified to

$$\frac{\Gamma(1 - (\alpha_i + \tilde{\alpha}_i))}{\Gamma(-(\alpha_i + \tilde{\alpha}_i))\Gamma(2)} = \frac{-(\alpha_i + \tilde{\alpha}_i)}{\Gamma(2)} \frac{\cancel{\Gamma(-(\alpha_i + \tilde{\alpha}_i))}}{\cancel{\Gamma(-(\alpha_i + \tilde{\alpha}_i))}}. \tag{6}$$

Hence, $D(\alpha + \tilde{\alpha}, 1)$ becomes

$$D(\alpha + \tilde{\alpha}, 1) = \begin{bmatrix} \frac{-(\alpha_1 + \tilde{\alpha}_1)}{\Gamma(2)} & 0 & \dots & 0 \\ 0 & \frac{-(\alpha_2 + \tilde{\alpha}_2)}{\Gamma(2)} & \dots & 0 \\ & \vdots & \ddots & \\ 0 & & & 0 \\ 0 & 0 & \dots & \frac{-(\alpha_n + \tilde{\alpha}_n)}{\Gamma(2)} \end{bmatrix}.$$

By equating the diagonal entries of $L_2P_2^{-1}$ to the diagonal entries of $D(\alpha+\tilde{\alpha},1)$, we solve for $\tilde{\alpha}$ and obtain the result.

Proof of Proposition 3: We start by invoking Gershgorin's theorem [33] and the reverse triangle inequality, which combine to say that for all $\lambda \in \sigma(A+\tilde{A}-D(\alpha,1))$ there exists a positive integer $i \in \{1,\dots,n\}$ such that the following holds $|\lambda| \leq |a_{i,i}+\tilde{a}_{i,i}-\psi(\alpha_i,1)| + \sum_{j\in N\setminus\{i\}} |a_{i,j}+\tilde{a}_{i,j}|$.

Hence, in providing sufficient graphical conditions to solve $\mathbf{P}_1^c$, we seek to find all $\tilde{a}_{i,j}$, for all $i \in \{1,\dots,n\}$ and $j \in \{1,\dots,n\}$ such that $|a_{i,i}+\tilde{a}_{i,i}-\psi(\alpha_i,1)| + \sum_{j\in N\setminus\{i\}} |a_{i,j}+\tilde{a}_{i,j}| < 1$. This implies that

$$\left|a_{i,i}+\tilde{a}_{i,i}-\frac{\Gamma(1-\alpha_i)}{\Gamma(-\alpha_i)\Gamma(2)}\right| < 1-\sum_{j\in N\setminus\{i\}} |a_{i,j}+\tilde{a}_{i,j}|. \quad (7)$$

Interestingly, we notice that the sufficient graphical constraint in (7) implicitly requires that $1-\sum_{j\in N\setminus\{i\}}|a_{i,j}+\tilde{a}_{i,j}| > 0$, which shows that the problem may not always be feasible. By the same relationship used in (6), the term $\frac{\Gamma(1-\alpha_i)}{\Gamma(-\alpha_i)\Gamma(2)}$ reduces to $\frac{\alpha_i}{\Gamma(2)}$.

Proof of Proposition 4:

Similar to the proof of Proposition 3, we again start by invoking Gershgorin's theorem [33] and the reverse triangle inequality, which combine to say that for all $\lambda \in \sigma(A-D(\alpha+\tilde{\alpha},1))$ there exists a positive integer $i \in \{1,\dots,n\}$ such that the following holds $|\lambda| \leq |a_{i,i}-\psi(\alpha_i+\tilde{\alpha}_i,1)| + \sum_{j\in N\setminus\{i\}} |a_{i,j}|$.

Hence, in providing sufficient graphical conditions to solve $\mathbf{P}_2^c$, we seek to find $\tilde{\alpha}_i$, for all $i \in \{1,\dots,n\}$ and $j \in \{1,\dots,n\}$ such that $|a_{i,i}-\psi(\alpha_i+\tilde{\alpha}_i,1)| + \sum_{j\in N\setminus\{i\}} |a_{i,j}| < 1$, which implies that

$$\left|a_{i,i}-\frac{\Gamma(1-(\alpha_i+\tilde{\alpha}_i))}{\Gamma(-(\alpha_i+\tilde{\alpha}_i))\Gamma(2)}\right| < 1-\sum_{j\in N\setminus\{i\}} |a_{i,j}|. \quad (8)$$

The sufficient graphical constraint in (8) implicitly requires that $1-\sum_{j\in N\setminus\{i\}}|a_{i,j}| > 0$. Therefore, the problem may not always be feasible. By the same relationship used in (6), the term $\frac{\Gamma(1-(\alpha_i+\tilde{\alpha}_i))}{\Gamma(-(\alpha_i+\tilde{\alpha}_i))\Gamma(2)}$ reduces to $\frac{(\alpha_i+\tilde{\alpha}_i)}{\Gamma(2)}$.

REFERENCES

[1] C. E. Begley and T. L. Durgin, "The direct cost of epilepsy in the United States: a systematic review of estimates," *Epilepsia*, vol. 56, no. 9, pp. 1376–1387, 2015.

[2] "Epilepsy: a public health imperative," 2019, last accessed March 17, 2022. [Online]. Available: https://www.who.int/publications/i/item/epilepsy-a-public-health-imperative

[3] A. Li, C. Huynh, Z. Fitzgerald, I. Cajigas, D. Brusko, J. Jagid, A. O. Claudio, A. M. Kanner, J. Hopp, S. Chen *et al.*, "Neural fragility as an EEG marker of the seizure onset zone," *Nature Neuroscience*, vol. 24, no. 10, pp. 1465–1474, 2021.

[4] D. Sritharan and S. V. Sarma, "Fragility in dynamic networks: application to neural networks in the epileptic cortex," *Neural Computation*, vol. 26, no. 10, pp. 2294–2327, 2014.

[5] J. P. Hespanha, *Linear Systems Theory*. Princeton Univ. Press, 2018.

[6] R. P. Agarwal, *Difference equations and inequalities: theory, methods, and applications*. CRC Press, 2000.

[7] A. Ashourvan *et al.*, "Model-based design for seizure control by stimulation," *J. Neural Engineering*, vol. 17, no. 2, Mar. 2020.

[8] S. Pequito *et al.*, "Spectral control of cortical activity," in *American Control Conference*, 2017, pp. 2785–2791.

[9] B. J. West, *Fractional Calculus View of Complexity: Tomorrow's Science*. Boca Raton, FL, USA: CRC Press, 2016.

[10] M. F. Shlesinger, G. M. Zaslavsky, and J. Klafter, "Strange kinetics," *Nature*, vol. 363, no. 6424, pp. 31–37, 1993.

[11] Y. Xue and P. Bogdan, "Constructing compact causal mathematical models for complex dynamics," in *Proceedings of the 8th International Conference on Cyber-Physical Systems*, 2017, pp. 97–107.

[12] S. Pequito, P. Bogdan, and G. J. Pappas, "Minimum number of probes for brain dynamics observability," in *54th IEEE Conference on Decision and Control*, 2015, pp. 306–311.

[13] B. N. Lundstrom, M. H. Higgs, W. J. Spain, and A. L. Fairhall, "Fractional differentiation by neocortical pyramidal neurons," *Nature Neuroscience*, vol. 11, no. 11, pp. 1335–1342, Oct. 2008.

[14] S. Thurner, C. Windischberger, E. Moser, P. Walla, and M. Barth, "Scaling laws and persistence in human brain activity," *Physica A: Stat. Mech. & Its App.*, vol. 326, no. 3–4, pp. 511–521, 2003.

[15] M. Scheffer *et al.*, "Early-warning signals for critical transitions," *Nature*, vol. 461, no. 7260, pp. 53–59, 2009.

[16] E. Reed, S. Chatterjee, G. Ramos, P. Bogdan, and S. Pequito, "Fractional cyber-neural systems—a brief survey," *Annual Reviews in Control*, 2022.

[17] E. A. Reed, P. Bogdan, and S. Pequito, "Quantification of fractional dynamical stability of EEG signals as a bio-marker for cognitive motor control," *Frontiers in Control Engineering*, 2022.

[18] A. O. Akdemir, H. Dutta, and A. Atangana, *Fractional order analysis: theory, methods and applications*. John Wiley & Sons, 2020.

[19] A. Dzielinski and D. Sierociuk, "Adaptive feedback control of fractional order discrete state-space systems," in *Proceedings of the International Conference on Computational Intelligence for Modelling, Control, and Automation*, 2005, pp. 804–809.

[20] M. De Oliveira, J. Geromel, and L. Hsu, "LMI characterization of structural and robust stability: the discrete-time case," *Linear Algebra and Its Applications*, vol. 296, no. 1-3, pp. 27–38, 1999.

[21] M. C. De Oliveira, J. Bernussou, and J. C. Geromel, "A new discrete-time robust stability condition," *Systems & Control Letters*, vol. 37, no. 4, pp. 261–265, 1999.

[22] E. J. Candès, J. Romberg, and T. Tao, "Robust uncertainty principles: Exact signal reconstruction from highly incomplete frequency information," *IEEE Transactions on Information Theory*, vol. 52, no. 2, pp. 489–509, 2006.

[23] J. B. Wagenaar, B. H. Brinkmann, Z. Ives, G. A. Worrell, and B. Litt, "A multimodal platform for cloud-based collaborative research," in *6th Inter. IEEE/EMBS Conf. on Neural Engineering*, 2013, pp. 1386–1389.

[24] E. A. Ihlen, "Introduction to multifractal detrended fluctuation analysis in Matlab," *Frontiers in Physiology*, vol. 3, p. 141, 2012.

[25] G. Gupta, S. Pequito, and P. Bogdan, "Dealing with unknown unknowns: Identification and selection of minimal sensing for fractional dynamics with unknown inputs," in *Proceedings of the Annual American Control Conference*, 2018, pp. 2814–2820.

[26] M. Grant and S. Boyd, "CVX: Matlab software for disciplined convex programming, version 2.1," http://cvxr.com/cvx, Mar. 2014.

[27] E. Beamer, W. Fischer, and T. Engel, "The ATP-gated P2X7 receptor as a target for the treatment of drug-resistant epilepsy," *Frontiers in Neuroscience*, vol. 11, p. 21, 2017.

[28] S. Chatterjee, O. Romero, A. Ashourvan, and S. Pequito, "Fractional-order model predictive control as a framework for electrical neurostimulation in epilepsy," *J. Neural Eng.*, vol. 17, no. 6, p. 066017, 2020.

[29] K. Deisseroth, "Optogenetics," *Nature Methods*, vol. 8, no. 1, pp. 26–29, 2011.

[30] M. Nedergaard, B. Ransom, and S. A. Goldman, "New roles for astrocytes: redefining the functional architecture of the brain," *Trends in Neurosciences*, vol. 26, no. 10, pp. 523–530, 2003.

[31] W. Rudin *et al.*, *Principles of Mathematical Analysis*. McGraw-Hill New York, 1964, vol. 3.

[32] S. Boyd, L. El Ghaoui, E. Feron, and V. Balakrishnan, *Linear Matrix Inequalities in System and Control Theory*. SIAM, 1994.

[33] R. S. Varga, *Geršgorin and his Circles*. Springer Science & Business Media, 2010, vol. 36.